Carbohydrate Polymers 90 (2012) 413–418

Contents lists available at SciVerse ScienceDirect

Carbohydrate Polymers

journal homepage: www.elsevier.com/locate/carbpol

Bacterial cellulose/silica nanocomposites: Preparation and characterization

Alireza Ashori[a,*], Somayeh Sheykhnazari[b], Taghi Tabarsa[b], Alireza Shakeri[c], Masood Golalipour[d]

[a] Department of Chemical Technologies, Iranian Research Organization for Science and Technology (IROST), P.O. Box 15815-3538, Tehran, Iran
[b] Department of Wood and Paper Technology, Gorgan University of Agricultural Sciences & Natural Resources, Gorgan, Iran
[c] Department of Chemistry, University of Golestan, Gorgan, Iran
[d] Department of Biology, University of Golestan, Gorgan, Iran

ARTICLE INFO

Article history:
Received 6 March 2012
Received in revised form 16 May 2012
Accepted 19 May 2012
Available online 27 May 2012

Keywords:
Bacterial cellulose
Tetraethoxysilane (TEOS)
Nanocomposite
Young's modulus
FE-SEM

ABSTRACT

The preparation and characterization of bacterial cellulose (BC)/silica nanocomposites are presented in this paper. BC hydro-gel was immersed in an aqueous solution of tetraethoxysilane (TEOS). By pressing the treated BC matrices at 120 °C and 2 MPa, water-free translucent sheets were obtained. TEOS concentration (3, 5 and 7%) and press time (8, 10 and 12 min) were used as variable factors. These materials were characterized by different techniques, namely FE-SEM, FTIR, SEM, tensile strength and Young's modulus. All composites showed good dispersion of the fibers and strong adhesion between the fibers and the matrix. FE-SEM observations showed that the nano-scale silica was embedded between the voids and micro-fibrils of the BC matrix. Reflecting this structure, the maximum Young's modulus and tensile strength of dry BC/silica composites improved to 1.46 GPa and 113 MPa, respectively. The tensile strength and Young's modulus showed 35 and 18-fold increase (with 7% TEOS), respectively, while the same properties were reduced 15 and 10-fold with increase in press time from 8 to 12 min. FTIR results illustrated strong chemical interactions between the cellulose and silica phases. The optimum condition was obtained when the TEOS dosage and press time were 7% and 8 min, respectively.

1. Introduction

Today, due to the global demand for fibrous materials, worldwide shortage of wood biomass in many areas, and environmental awareness, bacterial cellulose (BC) has become one of the promising alternative sources of fibrous materials for the 21st century (Sun, Yang, & Wang, 2010; Wan et al., 2009). In recent years, a great deal of interest has been generated for the production of cellulose using biotechnology method, which reduces the environmental impact to a minimum. Studies suggest that BC may be a better choice for manufacturing cellulose products (Castro et al., 2011; Czaja, Romanovicz, & Malcolm Brown, 2004), since BC is produced in a pure (free of impurities such as lignin and extractives) and crystalline form, which makes its recovery relatively simple. In terms of chemical structure, BC is identical to that produced by plants. However, it exhibits higher crystallinity, water-holding capacity, degree of polymerization, and mechanical strength (Darder, Aranda, & Ruiz-Hitzky, 2007; Sheykhnazari, Tabarsa, Ashori, Shakeri, & Golalipour, 2011). These properties make BC an interesting biomaterial for applications as nutritional component (Sani & Dahman, 2010), artificial skin (Hungund & Gupta, 2010), flexible display screens (Nakagaito, Nogi, & Yano, 2010), and in traditional applications where plant cellulose is used (Castro et al., 2011).

Historically, plant derived cellulose has been used either as reinforcement (Ashori & Nourbakhsh, 2010; Mottershead & Eichhorn, 2007; Nourbakhsh, Karegarfard, Ashori, & Nourbakhsh, 2010) or matrix (Darder et al., 2007), or as the sole component to prepare all-cellulose composites (Soykeabkaew, Arimoto, Nishino, & Peijs, 2008). Recently, BC has been used as reinforcement for various composites due to its excellent mechanical performance (Ifuku et al., 2007; Nakagaito, Iwamoto, & Yano, 2005; Sun et al., 2010). For instance, Gindl and Keckes (2004) prepared cellulose acetate butyrate based composites reinforced with BC sheets. Yano et al. (2005) demonstrated the production of nanocomposites made with BC nanofibers and acrylic resin. High-strength BC/phenolic resin composites were produced by Nakagaito et al. (2005). Hu et al. (2009) evaluated the bacterial cellulose nanofiber-reinforced unsaturated polyester resin composites.

Nanofibers and nanocomposite materials have gained much interest due to their remarkable change in properties. These materials can be combined effectively to obtain a new class of high performance or highly functional organic–inorganic hybrid materials. In recent years, cellulose-based nanocomposites have definitely proved their exceptional potential by providing a possibility of synthesizing a significant number of new nanomaterials with high degree of homogeneity and purity at molecular level and with extraordinary physical and chemical properties (Xie, Yu, & Shi,

* Corresponding author. Tel.: +98 21 5627 6637; fax: +98 21 5627 6265.
E-mail address: ashori@irost.org (A. Ashori).

0144-8617/$ – see front matter © 2012 Elsevier Ltd. All rights reserved.
http://dx.doi.org/10.1016/j.carbpol.2012.05.060

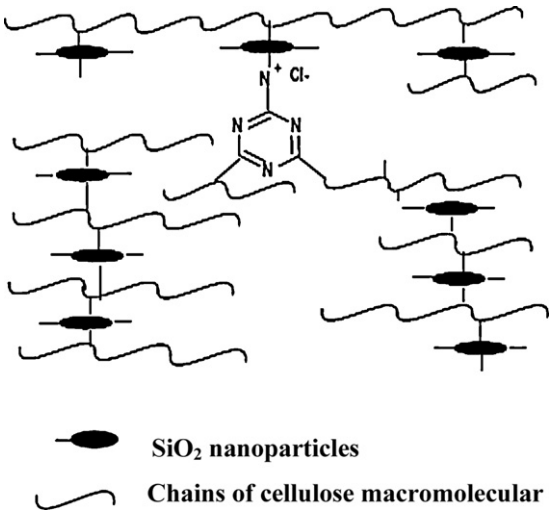

Fig. 1. Schematic model of cellulose/silica covalent crosslinking materials (Xie, Yu, et al., 2009).

2009). The reaction process involves the hydrolysis of silica precursors and condensation of the resulting hydroxyl groups to form a nanostructure. One simple method is mixing organic compounds with a metal alkoxide, such as tetraethoxysilane (TEOS). During the process, the inorganic mineral is deposited in the organic compound matrix forming hydrogen bonding between the organic and inorganic phases (Fig. 1). The BC fiber is one of the excellent natural biomaterials. BC has been explored as a substrate for composite materials because of the presence of several functional groups that may be employed in various activation processes. Chemical modification of BC can change its chemical and morphological structures for different purposes (Hou, Wang, & Yu, 2009; Xie, Zhang, & Yu, 2009).

The present study describes the preparation and characterization of nanocomposite materials obtained using BC and silica. In addition, the effects of TEOS and press time on the morphological and mechanical properties of BC-based nanocomposites have been investigated.

2. Materials and methods

2.1. Materials

The organism used was *Gluconacetobacter xylinus* (BPR 2004), which was obtained from the DSMZ Laboratory, Germany. The preparation procedures of BC were reported elsewhere (Sheykhnazari et al., 2011). In brief, *G. xylinus* was incubated in a static Hestrin–Schramm culture at 28 °C for 14 days. The obtained gel-like BC pellicles, about 6-mm thick, were purified by immersion in deionized water at 90 °C for 2 h and then boiled in a 0.5 M aqueous solution of NaOH for 15 min. The BC pellicles were then washed with deionized water several times and soaked in 1% NaOH for 2 days. Subsequently, the BC pellicles were washed free of alkali. Finally, a tridimensional network of nano- and micro-fibrils of BC with 10–100 nm width was obtained.

TEOS was used as a precursor. It was an analytical grade from Merk Co., Germany.

Table 1
Two variable factors and their combinations used in this study.

Press time (min)	TEOS (%)	Treatment
8	3	A1
10	3	A2
12	3	A3
8	5	B1
10	5	B2
12	5	B3
8	7	C1
10	7	C2
12	7	C3

2.2. Preparation of BC/silica nanocomposites

The BC/silica composite samples were prepared by the solution impregnation method. A certain amount of TEOS was mixed with 100 g of water together with 0.5 mL acetic acid (0.1N), and the mixture was stirred for 1 h. In order to control the silica content in BC gel, TEOS concentration in water was varied, i.e. 3, 5, 7%. BC gels were immersed in the TEOS solution and allowed to stand for 2 days. At high concentration of TEOS, brittle BC/silica mats were obtained. Subsequently, all surfaces of samples were wiped off with a dry cloth. Dry translucent BC/silica sheets were obtained by pressing BC/silica mats at 120 °C and 2 MPa. The process of preparation of the BC/silica composite is shown in Fig. 2. Experimental schedule is shown in Table 1. As it can be seen, the two variable factors were TEOS concentration and press time.

2.3. Sample characterization

The particle size of silica was investigated by a field emission-scanning electron microscope (FE-SEM, Hitachi 4160) with an accelerating potential of 15 kV. Scanning electron

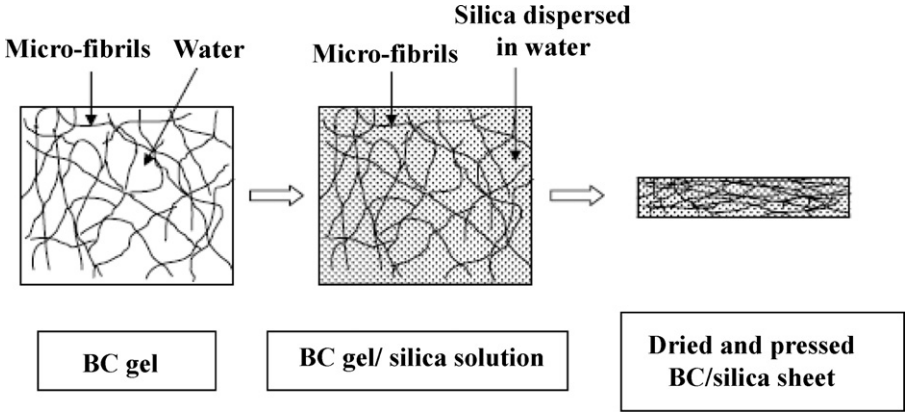

Fig. 2. Preparation process of dry and pressed BC/silica sheets from BC gels (Maeda et al., 2006).

microscopy (SEM) was used to observe the microorganism morphology and its distribution in the composite. A CamScan MV2300 SEM operating at 15 kV was used. Before scanning, each sample was coated with gold to improve its interface conductivity.

2.4. Fourier transform infrared spectroscopy (FTIR)

FTIR spectroscopy was used primarily to identify the chemical structure of the BC and BC/silica composites. Infrared absorption spectra were obtained from 4000 to 400 cm^{-1} using KBr pellets in a PerkinElmer spectrometer, model 2000.

2.5. Mechanical testing

Test specimens of 30 mm length and 10 mm width were cut from composite sheets. All specimens were equilibrated in a chamber kept at 20 °C and 35% relative humidity for 24 h before testing. The tensile strength of the plain matrix and all composites was measured by employing ASNTM STM universal tensile machine following ASTM D 5937-1996. The crosshead speed was set at 5 mm/min. All tests were conducted at ambient temperature and an average value of four repeated tests was taken for each treatment.

2.6. Statistical analysis

The experimental design consisted of two treatments (including TEOS concentration and press time) and their interactions. Data for each treatment was statistically studied by analysis of variance (ANOVA). When the ANOVA indicated a significant difference among factors and levels, a comparison of the means was done, employing Duncan's multiple range test (DMRT), to identify the groups that were significantly different from other groups at 99% and 95% confidence levels.

3. Results and discussion

3.1. Microstructure

A set of selected SEM micrographs of the surface of BC and BC/silica composite materials was studied. Representative SEM micrographs are shown in Fig. 3. For each material, the BC fibers dispersion and the interfacial adhesion are shown. Obviously, in the case of BC, only the small mat fragments, and not the isolated fibrils, were observed (Fig. 3a). Fig. 3b shows the surface of pressed and dried BC/silica sheets. The SEM micrographs provided evidence of the strong interfacial adhesion between the BC fibers and the matrix, as shown by the good dispersion within the matrix, without noticeable aggregates. As mentioned before, BC gel was immersed into aqueous solution of TEOS and silica was finally deposited on BC micro-fibrils via silanol. It is known that silanol is reactive and reacts with hydroxyl groups on organic polymers such as poly(vinyl alcohol), or polydimethylsiloxane having hydroxyl groups on both chain ends in organic–inorganic hybrids (cited by Maeda, Nakajima, Hagiwara, Sawaguchi, & Yano, 2006). Therefore, BC micro-fibrils having free hydroxyl groups may undergo condensation reactions with supplied silanol, which becomes fixed to micro-fibrils. Silanol itself also condenses forming silica, and is deposited on BC microfibrils through hydrogen bonding or condensation reactions with cellulose. These results clearly corroborated the superior mechanical properties of the BC/silica composites compared with BC material, as suggested by the mechanical tests discussed by Maeda et al. (2006).

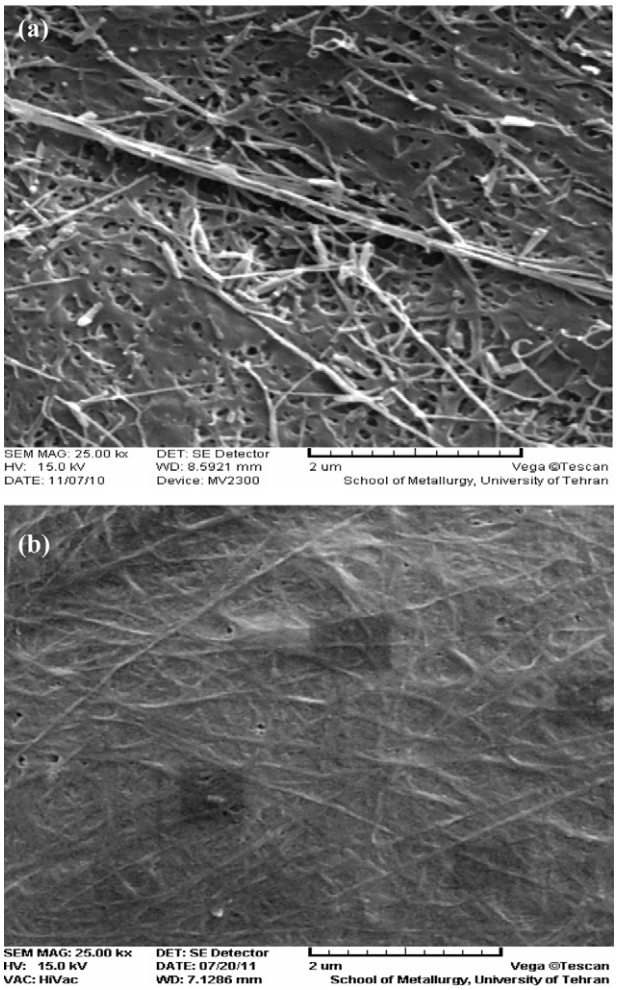

Fig. 3. SEM images of (a) BC micro-fibrils and (b) BC/silica composite.

FE-SEM analysis of the BC/silica composites was used to characterize the distribution of silica particles on the BC micro-fibrils (Fig. 4a) and the particle size of silica (Fig. 4b). Fig. 4a shows that there were a lot of silica particles on the composites surface. As mentioned earlier, BC was immersed in a silanol sol prepared from TEOS dispersed in water using acetic acid as a catalyst. Silica particles were deposited on the spaces/voids between BC nano- and micro-fibrils.

3.2. FTIR spectroscopy

Table 2 summarizes all FTIR results for BC, amorphous silica and BC/silica composites. Fig. 5 shows FTIR spectra obtained from three representatives BC/silica composites including A1, B1 and C1. As it can be seen in Table 2, there are some differences between the BC and BC/silica FTIR results that may be related to the strong chemical interactions between the cellulose and silica phases. The important changes among the spectra presented in Fig. 5a–c can be assigned to: 3200–3700 cm^{-1} (Si—OH), 1110–830 cm^{-1} (Si—O), and 460 cm^{-1} (Si—O—Si). This result is in good agreement with the works previously reported by Barud et al. (2008) and De Salvi, Barud, Caiut, Messaddeq, and Ribeiro (2012).

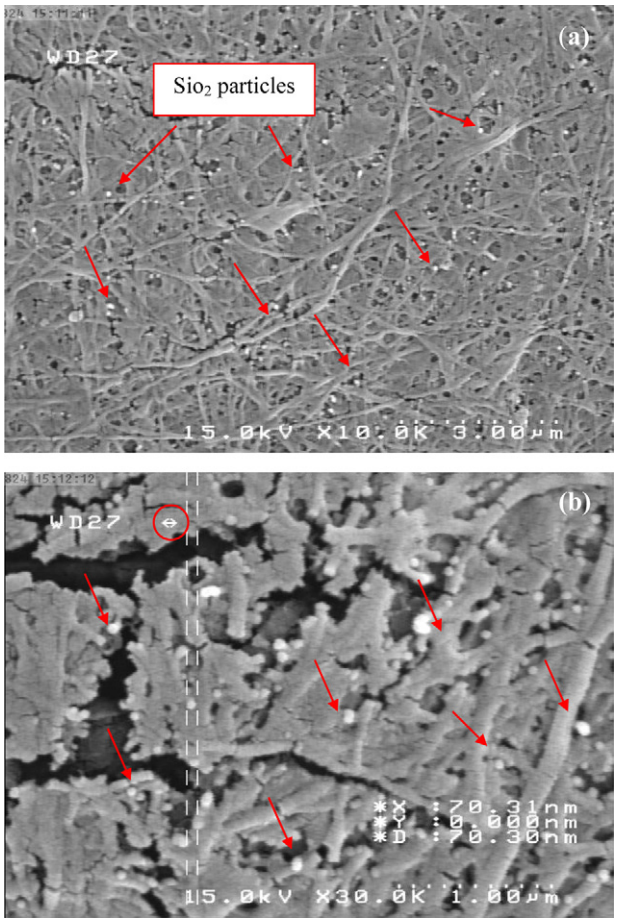

Fig. 4. FE-SEM micrographs (a) distribution of silica particles on the BC micro-fibrils and (b) nanoparticles of silica.

Table 2
FTIR results for BC, silica and BC/silica nanocomposite.

Assignment	Wavenumber (cm^{-1})		
	BC	Silica	BC/silica
O—H bending	400–700		
b-Glucosidic linkages between the glucose units	~896		
C—O symmetric stretching of primary alcohol	1040		
C—O—C antisymmetric bridge stretching	1168		
C—H deformation	1340		
CH_2 bending or O—H in plane bending	1400		
H—O—H bending of absorbed water	1650		
CH_2	2700		
CH stretching of CH_2 and CH_3 groups	2900		
H-bond	3246		
OH stretching	3500		
Si—O—Si bending		462	
Si—O—Si symmetric stretching		804	
Si—OH stretching		949	
Si—O stretching		1110	
Water OH bending		1640	
Water and silanol OH stretching		3460	
OH stretching			3300
C—H stretching			2900
Water OH bending			1640
CH_2 bending			1400
C—O—C bond			1160
O—H out-of-phase bending			600
Si—O—Si bending			460

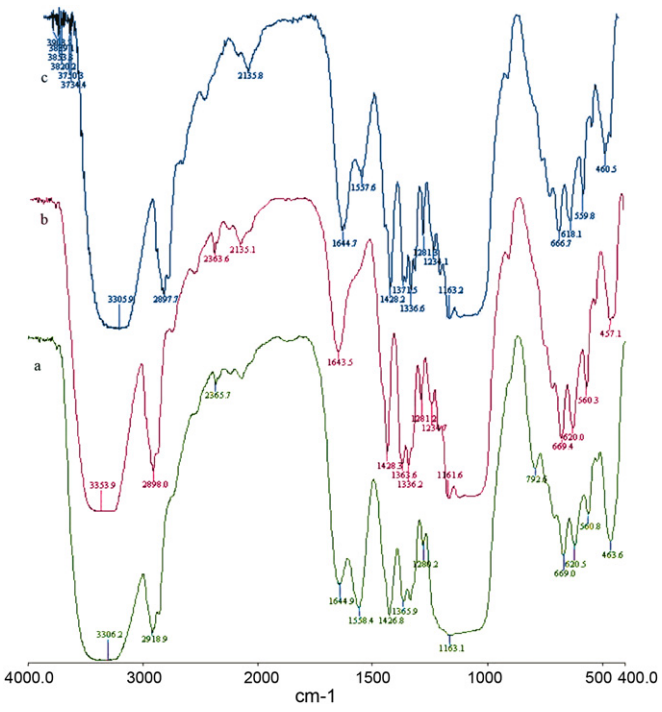

Fig. 5. FTIR spectra: (a) BC/silica 3%, (b) BC/silica 5% and (c) BC/silica 7%.

3.3. Mechanical properties

The most crucial factor that affects the mechanical properties of the composite materials is the fiber matrix interfacial adhesion. The quality of interfacial bonding is determined by several factors, such as the nature of filler and polymer components, the fiber aspect ratio, the processing procedure and the filler treatment (Nourbakhsh et al., 2010).

Statistical analysis showed that the mechanical properties in terms of tensile strength and Young's modulus of the samples were significantly influenced by the TEOS concentration and press time (Table 3). However, the interaction of variable factors was not significant. According to the DMRT, the differences between the mean values of the studied properties within and among each of the groups compared, were significant. For easier comparison between the mechanical performances of the various composites, the results are presented in Fig. 6. As clearly seen, all samples (group C) made with 7% TEOS had the highest values among the other types of specimens. In addition, both mechanical properties were decreased when the press time was increased from 8 to 12 min. With increase in press time, more heat can be transferred to the sheet, which would degrade the crosslinking between BC and TEOS. In addition, an increasing trend in tensile properties with silica content is found from Fig. 6. The superior mechanical properties of composites filled with 7% TEOS compared with those filled with 3 and 5% TEOS, confirmed the good interfacial adhesion and the strong interactions between the silica and the BC matrix. It is well accepted that tensile strength and Young's modulus of composites are influenced by the nature of matrix and the adhesion between fiber and matrix. Similar results have been reported by Xie, Yu, and Shi (2009) who studied the properties of cellulose/silica hybrid nanocomposites. Their data showed that the incorporation of nanoscale particles into cellulose matrix leads to a strong interfacial interaction.

Table 3
Results of ANOVA test on the effect of variables and their interaction on the mechanical properties.

Source of variations	df	Tensile strength			Tensile modulus		
		SS	MS	*F*	SS	MS	*F*
A	2	4571.97	2285.98	48.5**	0.233845	0.117	29.745**
B	2	1159.04	579.02	12.28**	0.047639	0.024	6.06*
A × *B*	4	9.20	2.3	0.049ns	0.007533	0.002	0.479ns
Error	18	848.41	47.14		0.070755	0.003931	
Total	26	6587.62			0.359773		

Note: *A* = TEOS concentration; *B* = press time; df = degree of freedom; MS = mean of squares; SS = sum of squares; *F* = *F* value; ns = not significant.
** Significant difference at the 1% level ($p \leq 0.01\%$).
* Significant difference at the 5% level ($p \leq 0.05\%$).

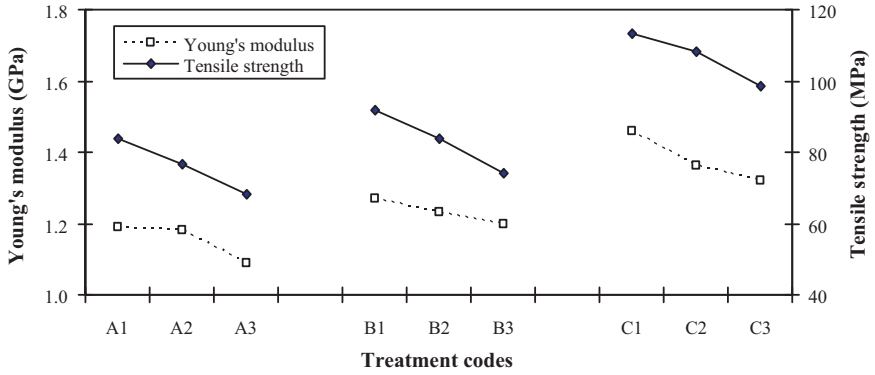

Fig. 6. Effects of TEOS concentration and press time on the mechanical properties.

4. Conclusions

The morphological and mechanical properties of BC/silica composites were evaluated to determine the influences of TEOS concentration (3, 5 and 7%) and press time (8, 10 and 12 min). Some conclusions are as follows:

a) In the present study, BC gel was immersed into aqueous solution of TEOS and silica was finally deposited on BC micro-fibrils via silanol.
b) The scanning micrographs provided evidence of the strong interfacial adhesion between the BC fibers and the matrix, as shown by the good dispersion within the matrix, without noticeable aggregates. This was attributed to the chemical bonding on the fiber–matrix interface under the function of TEOS coupling agent.
c) A decrease in both mechanical properties is observed for all composites when press time is increased from 8 to 12 min.
d) The tensile strength and Young's modulus increased by 35 and 18 fold (with 7% TEOS), while the same properties showed 15 and 10 fold reduction with increase in press time from 8 to 12 min, respectively.
e) Among the various formulations, composites C1 (7% TEOS and 8 min press time) had the maximum improvement in both mechanical properties.
f) FTIR spectra showed some differences between the BC and BC/silica samples, which is related to the chemical interactions between the cellulose and silica phases.
g) Finally, it was found that deposited nanoparticles of silica between BC nano- and micro-fibrils reinforced the composite.

References

Ashori, A., & Nourbakhsh, A. (2010). Reinforced polypropylene composites: Effects of chemical compositions and particle size. *Bioresource Technology*, *101*(7), 2515–2519.

Barud, H. S., Assunção, R. M. N., Martines, M. A. U., Dexpert-Ghys, J., Marques, R. F. C., Messaddeq, Y., et al. (2008). Bacterial cellulose–silica organic–inorganic hybrids. *Journal of Sol–Gel Science and Technology*, *46*(3), 363–367.

Castro, C., Zuluaga, R., Putaux, J.-L., Caro, G., Mondragon, I., & Gañán, P. (2011). Structural characterization of bacterial cellulose produced by *Gluconacetobacter swingsii* sp. from Colombian agroindustrial wastes. *Carbohydrate Polymers*, *84*(1), 96–102.

Czaja, W., Romanovicz, D., & Malcolm Brown, R. (2004). Structural investigation of microbial cellulose produced in stationary and agitated culture. *Journal of Cellulose*, *11*(3–4), 403–411.

Darder, M., Aranda, P., & Ruiz-Hitzky, E. (2007). Bionanocomposites: A new concept of ecological, bioinspired, and functional hybrid materials. *Advanced Materials*, *19*(10), 1309–1319.

De Salvi, D. T. B., Barud, H. S., Caiut, J. A., Messaddeq, Y., & Ribeiro, S. J. L. (2012). Self-supported bacterial cellulose/boehmite organic–inorganic hybrid films. *Journal of Sol–Gel Science and Technology*, http://dx.doi.org/10.1007/s10971-007-1669-9

Gindl, W., & Keckes, J. (2004). Tensile properties of cellulose acetate butyrate composites reinforced with bacterial cellulose. *Composites Science and Technology*, *64*(15), 2407–2413.

Hou, A., Wang, X., & Yu, Y. (2009). Preparation of the cellulose/silica hybrid containing cationic groups by sol–gel crosslinking process and its dyeing properties. *Carbohydrate Polymers*, *77*(2), 201–205.

Hu, L., Wan, Y., He, F., Luo, H. L., Liang, H., Li, X., et al. (2009). Effect of coupling treatment on mechanical properties of bacterial cellulose nanofibre-reinforced UPR ecocomposites. *Materials Letters*, *63*(22), 1952–1954.

Hungund, B. S., & Gupta, S. G. (2010). Strain improvement of *Gluconacetobacter xylinus* NCIM 2526 for bacterial cellulose production. *African Journal of Biotechnology*, *9*(32), 5170–5172.

Ifuku, S., Nogi, M., Abe, K., Handa, K., Nakatsubo, F., & Yano, H. (2007). Surface modification of bacterial cellulose nanofibers for property enhancement of optically transparent composites: Dependence on acetyl-group DS. *Biomacromolecules*, *8*(6), 1973–1978.

Maeda, H., Nakajima, M., Hagiwara, T., Sawaguchi, T., & Yano, S. (2006). Bacterial cellulose/silica hybrid fabricated by mimicking biocomposites. *Journal of Materials Science*, *41*(17), 5646–5656.

Mottershead, B., & Eichhorn, S. J. (2007). Deformation micromechanics of model regenerated cellulose fibre–epoxy/polyester composites. *Composites Science and Technology*, *67*(10), 2150–2159.

Nakagaito, A. N., Iwamoto, S., & Yano, H. (2005). Bacterial cellulose: The ultimate nano-scalar cellulose morphology for the production of high-strength composites. *Applied Physics A*, *80*, 93–97.

Nakagaito, A. N., Nogi, M., & Yano, H. (2010). Displays from transparent films of natural nanofibers. *MRS Bulletin*, *35*(3), 214–218.

Nourbakhsh, A., Karegarfard, A., Ashori, A., & Nourbakhsh, A. (2010). Effects of particle size and coupling agent on mechanical properties of particle-reinforced composites. *Thermoplastic Composite Materials*, *23*(2), 169–174.

Sani, A., & Dahman, Y. (2010). Improvements in the production of bacterial synthesized biocellulose nanofibres using different culture methods. *Journal of Chemical Technology and Biotechnology*, *85*(2), 151–164.

Sheykhnazari, S., Tabarsa, T., Ashori, A., Shakeri, A., & Golalipour, M. (2011). Bacterial synthesized cellulose nanofibers: Effects of growth times and culture mediums on the structural characteristics. *Carbohydrate Polymers*, *86*(3), 1187–1191.

Soykeabkaew, N., Arimoto, N., Nishino, T., & Peijs, T. (2008). All-cellulose composites by surface selective dissolution of aligned ligno-cellulosic fibres. *Composites Science and Technology*, *68*(10–11), 2201–2207.

Sun, D., Yang, J., & Wang, X. (2010). Bacterial cellulose/TiO_2 hybrid nanofibers prepared by the surface hydrolysis method with molecular precision. *Nanoscale*, *2*(2), 287–292.

Wan, Y. Z., Luo, H., He, F., Liang, H., Huang, Y., & Li, X. L. (2009). Mechanical, moisture absorption, and biodegradation behaviours of bacterial cellulose fibre-reinforced starch biocomposites. *Composites Science and Technology*, *69*(7–8), 1212–1217.

Xie, K., Yu, Y., & Shi, Y. (2009). Synthesis and characterization of cellulose/silica hybrid materials with chemical crosslinking. *Carbohydrate Polymers*, *78*(4), 799–805.

Xie, K., Zhang, Y., & Yu, Y. (2009). Preparation and characterization of cellulose hybrids grafted with the polyhedral oligomeric silsesquioxanes (POSS). *Carbohydrate Polymers*, *77*(4), 858–862.

Yano, H., Sugiyama, J., Nakagaito, A. N., Nogi, M., Matsuura, T., Hikita, M., et al. (2005). Optically transparent composites reinforced with networks of bacterial nanofibers. *Advanced Materials*, *17*(2), 153–155.